# Structure/property relationships for a series of crosslinked aromatic/aliphatic epoxy mixtures

**Jessica A. Schroeder, Patricia A. Madsen and Robert T. Foister**
*Polymers Department, General Motors Research Laboratories, Warren, Michigan 48090-9055, USA*
*(Received 1 May 1986; accepted 2 October 1986)*

Nine thermoset networks consisting of an aromatic epoxy novolac and an aliphatic epoxy, crosslinked with an imidazole catalyst, were investigated with the aim of correlating macroscopic behaviour and structure as network composition varied. The networks had properties ranging from the two extremes of the brittle, highly crosslinked aromatic, to the rubbery, less crosslinked aliphatic epoxy. The relationships between crosslink density, a measure of network microstructure, and both primary ($T_g$) and secondary ($T_\beta$) thermal transitions were investigated. These properties were also correlated with tensile toughness (stress/strain behaviour), strength and modulus. It was found that $T_g$ varied linearly with crosslink density whereas $T_\beta$ depended on the chemical composition of the network. Although no dependence of the room temperature modulus on crosslink density was found, both tensile strength and toughness were shown to change with crosslink density. Tensile toughness also exhibited a dependence on the temperature and frequency of the $\beta$-transition.

**(Keywords: thermoset networks; structure/property relationships; epoxies; crosslink density; thermal transitions)**

## INTRODUCTION

Thermosets based on crosslinked epoxies are used extensively as structural adhesives, matrix materials for fibre reinforced composites, coatings and potting compounds. The choice of particular pre-polymers, crosslinking agents, and thermal (processing) parameters, as well as fillers, diluents etc., is dictated by end-use, or service requirements. Given specific requirements, the usual approach is to formulate systems based on empirically derived guidelines. However, it is ultimately desirable to correlate microscopic characteristics, which for epoxy systems include crosslink density, free volume and thermal transitions, with macroscopic properties such as Young's modulus, stress relaxation, fracture toughness, moisture and/or solvent diffusion and fatigue crack resistance. These properties and relationships may then serve as the basis for a quantitative understanding relating end-use requirements to molecular structure.

It is the purpose of this work to investigate such structure/property relationships for a series of thermoset networks obtained by crosslinking epoxy novolac and aliphatic epoxy pre-polymers using a substituted imidazole as crosslinking agent. By varying the ratio of aromatic to aliphatic epoxy prepolymer, while keeping processing conditions constant, a variety of network structures and properties were obtained. The networks had properties ranging from the two extremes of the brittle, highly crosslinked novolac to the rubbery, less crosslinked aliphatic epoxy. Network structure, assessed through crosslink densities measured in the rubbery state, and thermal transitions (both the glass/rubber transition and structural transitions in the glassy state) were correlated with composition and with macroscopic properties such as stress/strain behaviour, yield and modulus.

## EXPERIMENTAL

### *Materials*

The materials used, suppliers, molecular weights and dispersities as determined by gel permeation chromatography, epoxy equivalent weights (*EEW*) and comments are listed in *Table 1*. The novolac, D.E.N. 431, and the reactive aliphatic epoxy, Epi-Rez 5048, were used as received. The curing agent, [1-(2-hydroxypropyl)-2-methylimidazole], AP-5, was distilled (145°C, 2 mm Hg) prior to use. The structure of D.E.N. 431 was provided by the supplier, while the structures of Epi-Rez 5048 and AP-5 were determined by nuclear magnetic resonance (see *Figure 1*).

### *Sample preparation*

Nine formulations were prepared from these materials, maintaining a ratio of imidazole crosslinking agent functionality to total epoxide functionality of 0.113. The weight per cents of aliphatic epoxy were varied systematically in the order 0, 19, 33, 43, 50, 57, 67, 80 and 100. In the text, formulations will be identified by a formulation number followed by, in parentheses, the weight per cent aliphatic epoxy, Epi-Rez 5048.

For each formulation the indicated amounts of aromatic and aliphatic epoxy were mixed and degassed at 100°C for five to six hours, mainatined under vacuum overnight, and then reheated to 100°C for four hours. This mixture was cooled and the appropriate amount of curing agent added under vacuum, after which the mixture was poured into a glass plate assembly to form sheets. This assembly consisted of two Frekote 44-treated Pyrex plates separated by rubber tubing, spaced with stainless steel shims and held together with binder clips. The system was then allowed to gel at room temperature.

0032-3861/87/060929-12$03.00

**Table 1** Materials

| Material | Supplier | EEW[a] | $\bar{M}_n$ | $\bar{M}_W$ | $\bar{M}_W/\bar{M}_N$ | Comment |
|---|---|---|---|---|---|---|
| D.E.N. 431 | Dow Chemical | 172–179 | 400 | 500 | 1.25 | Epoxy novolac resin |
| Epi-Rez 5048 | Celanese Plastics and Specialties | 145–165 | 400 | 400 | 1.00 | Aliphatic triglycidyl ether resin |
| AP-5 | Archem Corporation | — | 140 | — | — | 1-[2-Hydroxypropyl]-2-methylimidazole |

[a] EEW = Epoxy equivalent weight as provided by supplier

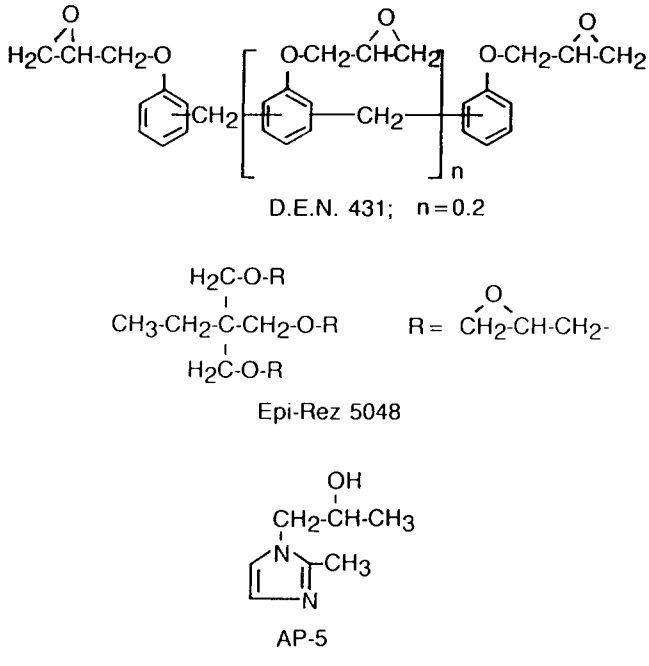


**Figure 1** Structures

After 24 h, it was further cured for 30 min at 150°C in a forced air oven, cooled to room temperature and demoulded. Sheets obtained from this procedure were approximately 3.8 mm thick.

Samples for the experiments described below were cut from the sheets to the desired geometry using a diamond saw and, when necessary, a Tensilkut router. All samples were then subjected to a post-cure cycle*.

*Chemical reaction rate constants and activation energies*

Rate constants and activation energies for the crosslinking reactions of formulations 1(0), 3(33), 7(67) and 9(100) were obtained using a DuPont 1090 Thermal Analyzer with a DuPont 912 DSC module. Small amounts of each formulation were hand mixed with an appropriate amount of the imidazole catalyst. Within two hours of mixing, 7 to 15 mg aliquots were hermetically sealed in aluminium pans and heated from room temperature through a cure exotherm at rates of 2, 5, 10, 15 and 20°C/min. The temperature of the maximum in the cure exotherm peak was recorded at each heating rate. Using these data, rate constants and activation energies of cure were calculated as described in ASTM E698.

*Density and thermal expansion measurements*

Room temperature densities were obtained by weighing and measuring dimensions of specimens (approximately 6.35 × 6.35 × 3.8 mm) cut from a sheet for each formulation. Mass to volume ratios were then calculated.

Thermal expansion data measured with a DuPont 990 Thermal Analyzer coupled with a 943 Thermomechanical Analyzer module (TMA) and Omnitherm Data System were used to find the densities of the samples at $T_g + 40°C$. Specimens, similar to the room temperature density specimens described above, were heated to a minimum of 40°C above $T_g$ at a rate of 10°C/min. Data were recorded as a linear dimension change vs. temperature. The per cent dimension change of the specimens from room temperature to $T = T_g + 40°C$ could then be obtained. Assuming that the samples expand isotropically, the volume of a specimen at $T_g + 40°C$ was calculated by adding the per cent dimension change (volume) to the room temperature volume. The high temperature density was then determined as the ratio of mass to volume at $T_g + 40°C$.

*Moduli*

*Room temperature modulus.* The tensile modulus of each of the nine formulations was obtained using an Instron (Model TTC) testing machine. Tensile dogbones were prepared and tested in accordance with ASTM D638. Specimens were pulled at room temperature, with an extensometer measuring elongation, at a rate of 5 mm/min, to a maximum strain of 10%. Load and elongation measurements were recorded on a strip chart. Room temperature moduli are reported as the ratio of stress to strain determined from the initial slope of the load vs. elongation curve. The maximum stress, or strength to break, was obtained from these data. Toughness values were calculated from the area under the load vs. elongation curve up to the break point. In some cases, yielding prior to break was apparent, yield being defined as the point where stress no longer increases with strain.

*High temperature equilibrium modulus.* Tensile samples prepared from each of the nine formulations were tested on an Instron Universal Testing Machine, model 1125, with attached environmental chamber and Microcon II data system. Each specimen was allowed to equilibrate for 30 min prior to testing in the environmental chamber, which was maintained at the test temperature. In each case, the test temperature was $T_g + 40°C$. Specimens were strained in small increments, with a strain gauge measuring elongation, at a rate of 0.5 mm/min, to a maximum strain of 5%. After each extension, the load was allowed to decay to an apparent constant equilibrium value. The equilibrium tensile modulus, $E_e$, was obtained from plots of the equilibrium stress vs. strain data. Stress/strain curves were reproducible, on average, within 5%. As described below, these data were used to characterize the crosslink density of each formulation.

* Post-cure cycle: 25 min at 200°C; 60 min at room temperature; 75 min at 160°C; cold water quench to room temperature; 30 min at 135°C; 60 min at room temperature; 20 min at 135°C; 60 min at room temperature; 40 min at 160°C; cool to room temperature.

*Glass transition temperature measurements*

*Differential scanning calorimetry* (D.s.c.) $T_g$'s of each of the nine formulations were obtained using a DuPont 990 Thermal Analyzer with a d.s.c. module. D.s.c. specimens (10–20 mg) cut from a sheet were heated to above $T_g$ at 10°C/min, quench cooled (−80°C/min), and reheated at 10°C/min. $T_g$ is reported as the temperature at the transition midpoint, i.e. the temperature at $(1/2)\Delta C_p$, where $\Delta C_p$ is the change in heat capacity during the transition. The widths of the transition (the difference between the temperature at the initial change of slope to the temperature at the final change of slope of the heat capacity) were 20°C–40°C. In all cases, data from the second heating scan are reported.

*Dynamic mechanical analysis (DMA).* $T_g$'s of each of the nine formulations were obtained using a DuPont 1090 Thermal Analyzer with a DuPont 982 DMA module. DMA specimens, 63.5 × 13.0 × 3.8 mm cut from a sheet of the appropriate formulation, were clamped in the module with a jaw separation of 40.0 mm. Each specimen was cooled to −150°C, allowed to equilibrate for about 8 min, and then heated through $T_g$ at 5°C/min. $T_g$ is reported as the temperature of the maximum in the tan $\delta$ vs. temperature curve.

*Glassy state (β) transitions*

*Dynamic mechanical thermal analysis (DMTA).* Dynamic storage moduli and damping (tan $\delta$) for each of the nine compositions were measured, as a function of temperature (−150°C to 100°C, at a heating rate of 2°C/min) with a dynamic mechanical thermal analyser (Polymer Laboratories, Inc.). The multiplexing capabilities of the instrument allowed measurement of material response for five discrete frequencies (0.33, 1.0, 3.0, 10.0, 30.0 Hz) at a fixed (±0.2°C) temperature. Rectangular specimens (5.0 × 0.9 × 0.17 cm) cut from sheets cast in the manner detailed above were constrained at both ends in a clamping fixture inside an environmental chamber. A drive clamp vibrated the centre of the specimen at the desired frequency, and the resultant strain was measured by a transducer.

## RESULTS

*Network microstructure*

*Crosslinking kinetics.* Differential scanning calorimetry, applied in accordance with ASTM E698, Appendix X3, was used to calculate Arrhenius activation energies and rate constants of the crosslinking reaction for formulations 1(0), 3(33), 7(67) and 9(100). The following equation, based on work by Kissinger[1], was used:

$$E = -R\left[\frac{\mathrm{d}\ln(B/T_{max}^2)}{\mathrm{d}(1/T_{max})}\right] \quad (1)$$

where $E$ is the activation energy, $R$ the gas constant, $B$ the heating rate and $T_{max}$ the absolute temperature of the reaction peak maximum for the heating rate, $B$. $B$ and $T_{max}$ are parameters determined from the d.s.c. scans. Activation energies can be obtained from plots of $-\ln(B/T_{max}^2)$ vs. $1/T_{max}$, which have slopes of $E/R$ (see *Figure 2*).

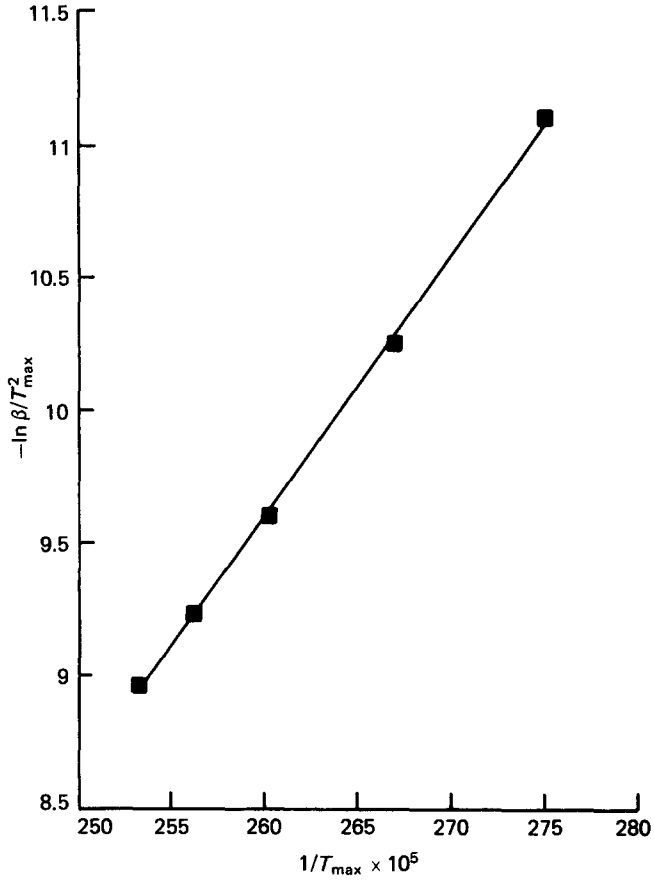


**Figure 2** Activation energy determination for formulation 9(100); slope = $E/R$

Once $E$ has been determined, the reaction rate constant at any temperature may be calculated from

$$k = Ze^{-E/RT} \quad (2)$$

where $k$ is the specific rate constant, $T$ the absolute temperature and the expression for $Z$ is[2]

$$Z = (BEe^{E/RT_{max}})/RT_{max}^2 \quad (3)$$

In equation (3), $Z$ is the pre-exponential factor and $B$ a heating rate, in this case 10°C/min.

Experiments were performed using formulations 1(0) and 9(100), the individual pre-polymers, and 3(33) and 7(67) as representative of the mixtures. Activation energies of 57.6, 74.5, 71.0 and 80.7 kJ mol$^{-1}$ were found for formulations 1(0), 3(33), 7(67) and 9(100), respectively. Rate constants at various temperatures may be calculated using equation (2). At low reaction temperatures, formulation 1(0) has the highest rate constants, while at higher temperatures (>373 K), formulation 9(100) has the highest rate constants.

*Crosslink density.* Simple rubber elasticity theory, along with the experimental equilibrium rubber modulus, was used to characterize the crosslink density of the epoxy materials through the following relationship[3]:

$$M_c = \phi\rho RT/G_e \quad (4)$$

where $M_c$ is the average molecular weight between crosslinks, $\phi$ the front factor, $\rho$ the density at absolute temperature $T$, $R$ the gas constant, and $G_e$ the equilibrium

shear modulus. A rubber is at equilibrium when, with a change in temperature, reversible changes of the elastic forces acting on the strained rubber occur[4]. In tensile experiments equilibrium can be achieved when, after deformation, the load and displacement of the rubber decay to apparent constants. A thorough discussion of rubber elasticity, including a derivation of equation (4), may be found in the work by Treloar[5]. In order to apply equation (4), modulus measurements are generally made at $T = T_g + 40°C$, since the behaviour of an epoxy network will then approximate the behaviour of a rubber. For a rubber experiencing small strains, volume is constant during deformation and $G_e$ may be replaced by $E_e/3$, which is one-third the equilibrium tensile modulus. The front factor, $\phi$, is the ratio of the mean square end-to-end distance of a network chain to that of a randomly coiled chain. In this work $\phi$ is assumed to be one[6]. The correction factor for free, unreacted chain ends, important for a network in the early stages of the crosslinking reaction[6,7], may be neglected here since all samples have been post-cured.

Thus, equation (4) may be written

$$E_e = 3\rho RT/M_c \quad (5)$$

or

$$\sigma/3\rho RT = \varepsilon/M_c \quad (6)$$

where $\sigma$ and $\varepsilon$ are the equilibrium stress and strain, respectively. Plots of $\sigma$ vs. $\varepsilon$ will have a slope of $1/M_c$, the inverse of the molecular weight between crosslinks, which can be identified with crosslink density. An example of such a plot is shown in *Figure 3*.

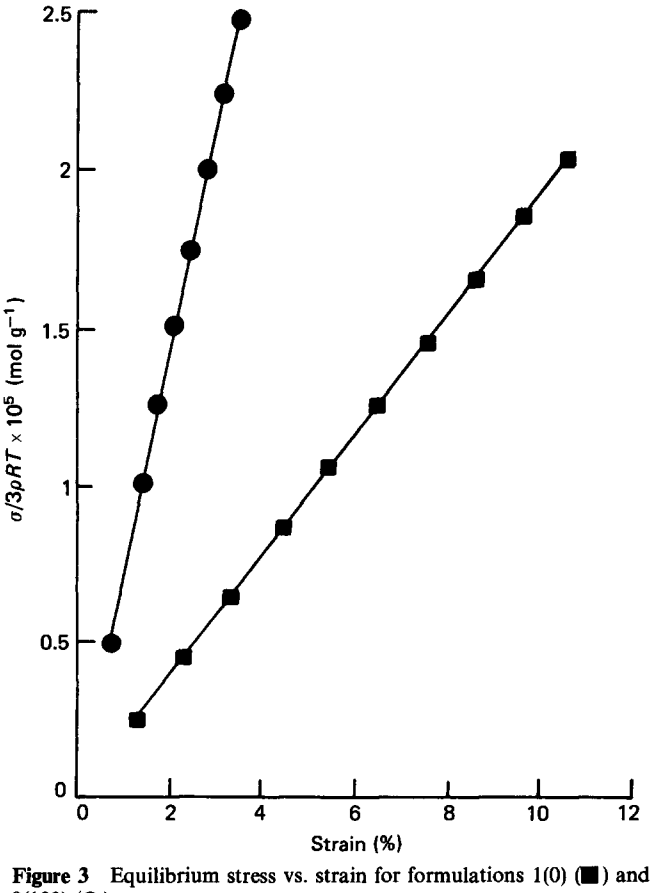


**Figure 3** Equilibrium stress vs. strain for formulations 1(0) (■) and 9(100) (●)

**Table 2** Parameters for determining crosslink density ($1/M_c$)

| Formulation | Test temperature[a] (°C) | $\rho_{RT}$ (g/cc) | $\rho_T$ (g/cc) | $M_c$ (g mol$^{-1}$) | $1/M_c$ ($\times 10^3$ mol g$^{-1}$) |
|---|---|---|---|---|---|
| 1(0) | 180 | 1.214 | 1.199 | 188 | 5.3 |
| 2(19) | 190 | 1.207 | 1.190 | 154 | 6.5 |
| 3(33) | 185 | 1.200 | 1.182 | 180 | 5.6 |
| 4(43) | 160 | 1.200 | 1.185 | 197 | 5.1 |
| 5(50) | 145 | 1.207 | 1.193 | 292 | 3.4 |
| 6(57) | 125 | 1.217 | 1.204 | 385 | 2.6 |
| 7(67) | 110 | 1.211 | 1.206 | 492 | 2.0 |
| 8(80) | 85 | 1.194 | 1.189 | 856 | 1.2 |
| 9(100) | 70 | 1.080 | 1.075 | 725 | 1.4 |

[a] Test temperature approximates $T_g$ (as determined by d.s.c.) + 40°C

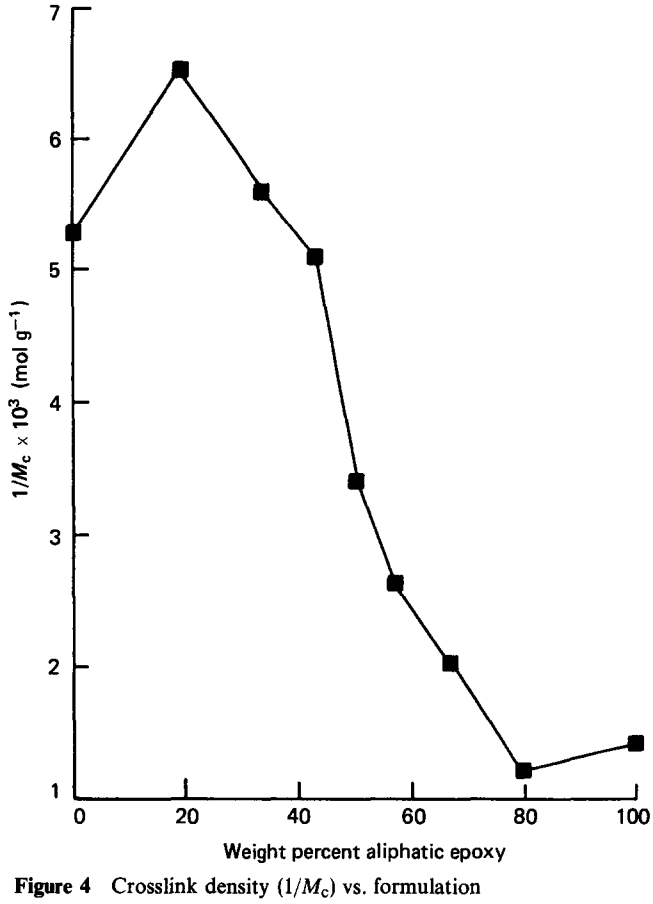


**Figure 4** Crosslink density ($1/M_c$) vs. formulation

The density at $T_g + 40°C$, the molecular weight between crosslinks, $M_c$, and the crosslink density, $1/M_c$, obtained for each of the nine formulations are listed in *Table 2*. $M_c$ ranges from 154 g mol$^{-1}$ (formulation 2(19)) to 856 g mol$^{-1}$ (formulation 8(80)). These $M_c$ values are within the same order of magnitude as values reported by Lemay *et al.*[3] for an amine cured diglycidyl ether of bisphenol A epoxy network. For formulations 1(0) and 9(100), the $M_c$ values correspond to $N_c$ values (number of monomer units between crosslinks) of 1.1 and 1.8, respectively. A plot of crosslink density, $1/M_c$, vs. formulation, *Figure 4*, shows a maximum crosslink density at formulation 2(19), and a minimum at formulation 8(80). Overall, as the amount of aliphatic epoxy in the formulation increases, the crosslink density decreases.

*Thermal transistions*

*Glass transitions.* For a thermoset, the glass transition temperature ($T_g$) marks the glass to rubber transition and is associated with long range cooperative motion of the crosslinked network. Modulus, toughness, extensibility and creep behaviour are influenced by this transition. $T_g$'s were obtained by d.s.c. for each of the nine formulations. Generally, as the amount of aliphatic epoxy in the formulations increases, $T_g$ decreases (*Figure 5*). There is, however, a maximum $T_g$ at formulation 2(19). To confirm this behaviour, $T_g$'s were obtained using DMA. As expected, since DMA is a dynamic technique and $T_g$ is frequency dependent, DMA $T_g$'s are higher than the corresponding d.s.c. $T_g$'s. However, the overall trend is the same, and the maximum occurs at formulation 2(19).

*Glassy state relaxations.* ($T_\beta$) A $\beta$-transition, which corresponds to the onset of localized (segmental) motion or side group motion, is defined as the highest temperature secondary, or glassy state (sub-$T_g$), relaxation in the network. The temperature of this relaxation and the nature of the relaxing group affect the diffusion of small molecules, such as water, within the network, as well as the impact toughness of the material. DMTA of the series of formulations shows a well-defined $\beta$-transition which occurs, depending on the particular frequency and composition, in the range of $-33$°C to $-80$°C. A typical DMTA plot of tan $\delta$ vs. temperature for three of the five test frequencies is shown in *Figure 6* (the glass transition region is not included). As can be seen in *Figure 7*, for a given frequency there is generally, over the composition range, a change of some 15°C to 20°C in $T_\beta$ (the temperature at the maximum of the tan $\delta$ peak). Generally both $T_\beta$ and the transition width increase with frequency for a given composition. Furthermore, *Figure 7*

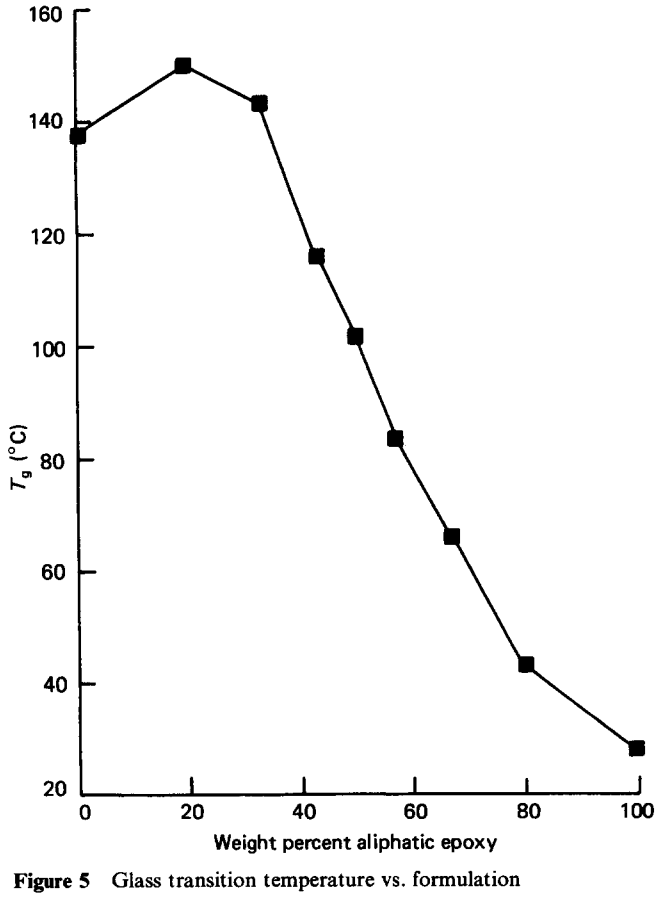


**Figure 5** Glass transition temperature vs. formulation

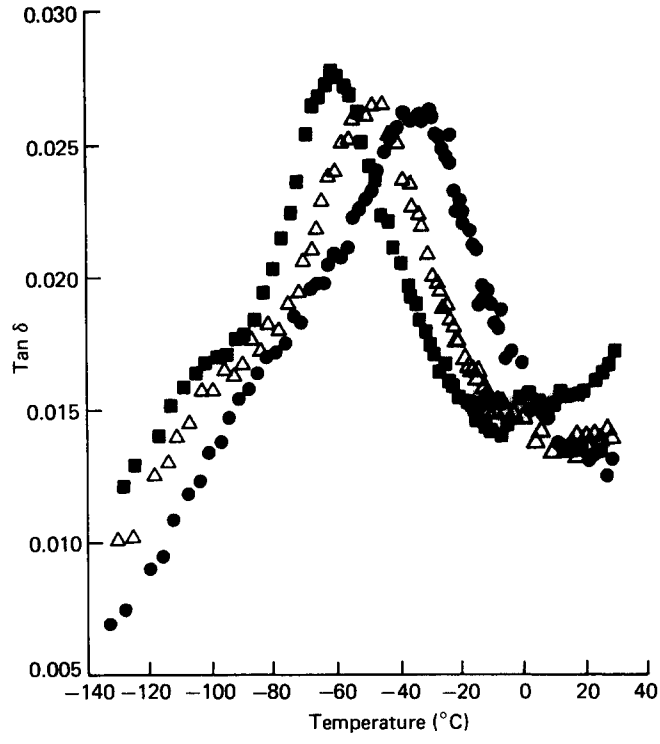


**Figure 6** Beta transitions (tan $\delta$ vs. temperature) for formulation 1(0) at 0.33 Hz (■), 3 Hz (△) and 30 Hz (●)

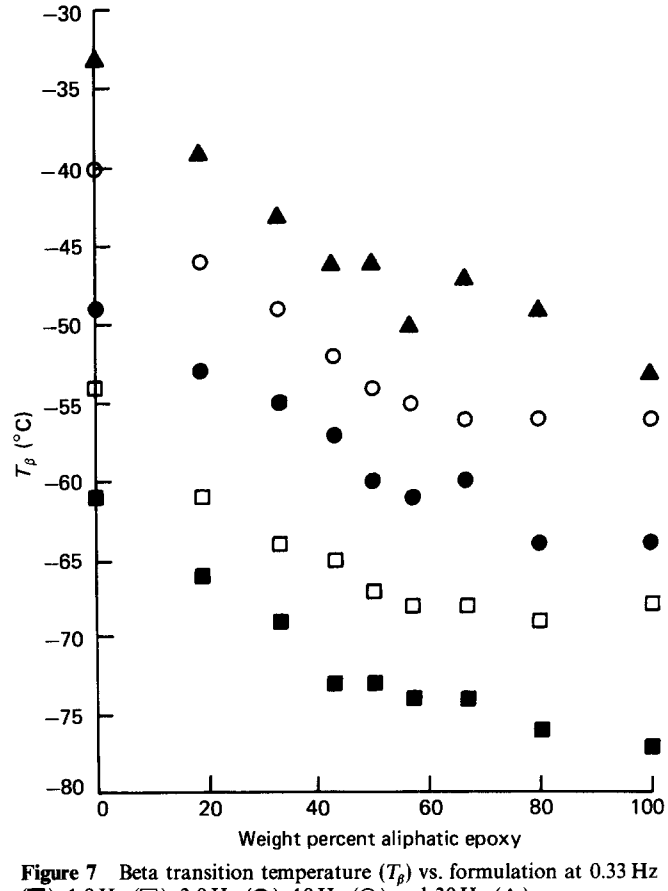


**Figure 7** Beta transition temperature ($T_\beta$) vs. formulation at 0.33 Hz (■), 1.0 Hz (□), 3.0 Hz (●), 10 Hz (○) and 30 Hz (▲)

indicates that $T_\beta$ decreases at all frequencies with increasing weight per cent aliphatic epoxy.

Activation energies for the $\beta$-transition, $E_{a,\beta}$, calculated from Arrhenius plots of ln $f$ vs. $1/T_\beta$, are given in *Table 3*. Literature values of $E_{a,\beta}$ reported for some other materials[8,9] have been included in the table for

**Table 3** Activation energies and entropies

| Formulation | Activation energy, $E_{a,\beta}$ (kJ mol$^{-1}$) | Activation entropy, $\Delta S_\beta{}^a$ (eu) |
|---|---|---|
| 1(0) | 68.0 | 14.8 |
| 2(19) | 65.6 | 12.4 |
| 3(33) | 65.1 | 11.6 |
| 4(43) | 63.2 | 11.3 |
| 5(50) | 63.6 | 10.7 |
| 6(57) | 67.3 | 10.4 |
| 7(67) | 65.2 | 10.4 |
| 8(80) | 61.3 | 10.1 |
| 9(100) | 66.5 | 10.4 |

PMMA 74.0
DGEBA/ethylenediamine 46.9
$^a$ 1 eu = 1 cal mol$^{-1}$ K$^{-1}$ = 4.18 J mol$^{-1}$ K$^{-1}$

**Table 4** Tensile modulus and break strength

| Formulation | Modulus (kPa × 10$^{-6}$) | Break strength (kPa × 10$^{-4}$) |
|---|---|---|
| 1(0) | 3.34±0.06 | 5.87±1.0 |
| 2(19) | 3.22±0.26 | 5.30±1.27 |
| 3(33) | 3.11±0.37 | 7.50±0.48 |
| 4(43) | 3.32±0.12 | 7.05±0.33 |
| 5(50) | 3.26±0.42 | 7.82±0.08 |
| 6(57) | 3.36±0.13 | 7.05±0.19 |
| 7(67) | 3.47±0.22 | 6.58±0.40 |
| 8(80) | 2.98±0.09 | 3.95±0.12 |
| 9(100) | 0.29±0.01 | 0.28±0.02 |

comparison. There is little apparent variation in $E_{a,\beta}$ with composition for the nine epoxy formulations. Using the values given in *Table 3*, we find a mean activation energy of 65.1±2.1 kJ mol$^{-1}$.

*Macroscopic properties*

*Tensile modulus.* The room temperature tensile modulus and strength to break were obtained for all nine formulations (*Table 4*). The room temperature modulus appears independent of composition for formulations 1(0) through 8(80), with a mean value of $3.26 \times 10^6$ kPa. Formulation 9(100) shows a significant drop in modulus, with a value of $2.9 \times 10^5$ kPa. The maximum stress, or strength to break (at room temperature), exhibits a maximum at formulation 5(50).

*Stress/strain behaviour (toughness).* Toughness was calculated from tensile load vs. elongation curves by measuring the area under the curve up to break. In some cases, a yield point was observed prior to break. Yield, the point at which stress decreases with strain, or ceases to increase with increasing strain, is an indication of plastic deformation. These data are listed in *Table 5*. The data for the more brittle formulations exhibit considerable scatter, and maximum toughness occurs at formulation 6(57).

## DISCUSSION

*Network structure*

*Influence of reaction rate.* In general the crosslinking mechanism, reaction rates and reaction conditions control the morphology, or microstructure, of the network that is ultimately obtained. For all nine formulations, network formation was a three step process: a 24 h room temperature gel; a 1/2 h, 150°C oven cure; and a post-cure cycle. Rate constants of the crosslinking reactions vs. reaction temperature were calculated (equation (2)) for the aromatic and aliphatic epoxies and two of the mixtures. The rate constant for formulation 1(0) (the aromatic epoxy novolac resin) is higher than the constant for formulation 9(100) (the aliphatic epoxy resin) at low temperatures, but is lower than the formulation 9(100) rate constant at high temperatures. When the calculated rate constants are plotted vs. temperature (*Figure 8*), the temperature at which rate crossover occurs is shown to be about 97°C for formulations 1(0) and 9(100). (The crossover points for formulations 1(0) and 3(33) and 1(0) and 7(67) are 106°C and 107°C, respectively.) Thus, during the first step of the crosslinking reaction, the room temperature gel, the aromatic epoxy reacts faster, and a greater degree of crosslinking is attained than for the aliphatic epoxy. During the oven cure step, according to these rate constants, the aliphatic epoxy should react faster. When samples of formulations 1(0) and 9(100) were first allowed

**Table 5** Toughness and yield strength

| Formulation | Toughness (J) | Yield strength (kPa × 10$^{-4}$) |
|---|---|---|
| 1(0) | 0.690±0.35 | – |
| 2(19) | 0.773±0.40 | – |
| 3(33) | 2.41±0.63 | – |
| 4(43) | 1.63±0.42 | – |
| 5(50) | 3.18±0.42 | – |
| 6(57) | 4.92±1.10 | 7.39±0.03 |
| 7(67) | 2.84±0.54 | 7.09±0.02 |
| 8(80) | 2.54±0.41 | 5.52±0.07 |
| 9(100) | 0.640±0.061 | – |

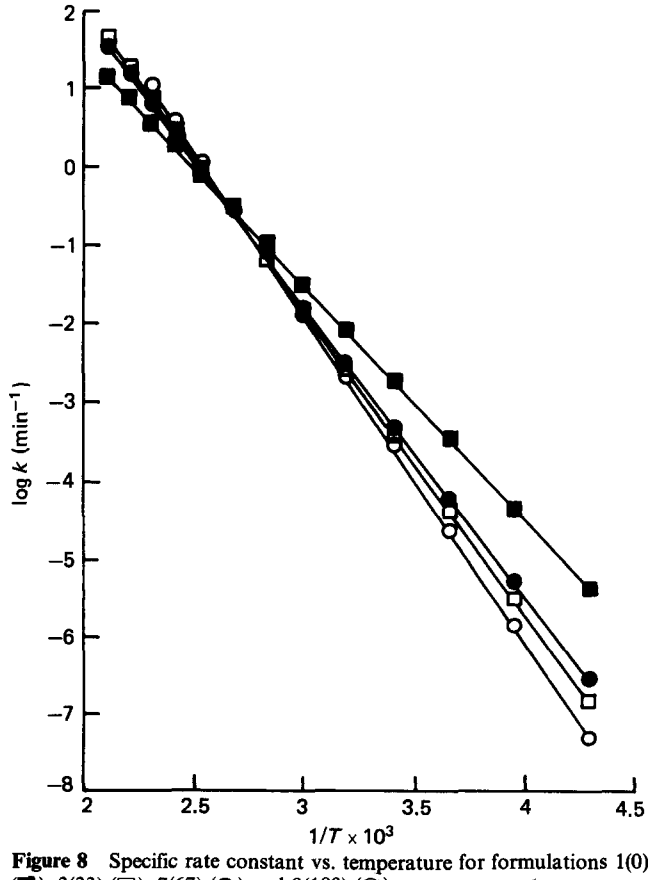


**Figure 8** Specific rate constant vs. temperature for formulations 1(0) (■), 3(33) (□), 7(67) (●) and 9(100) (○)

to gel at room temperature and rate constants were then obtained, the results were similar. That is, during the second step of network formation (oven cure) the aliphatic epoxy reacts faster than the aromatic epoxy. It appears, though, that the gel step, where the aliphatic epoxy reacts more slowly, is the more important step in determining the final network structure. That the aliphatic epoxy is generally slower to react is shown by the incomplete crosslinking of a formulation 9(100) sample even after the first high temperature post-cure cycle. It was found that if the 9(100) sample is post-cured a second time, the $T_g$ increases further.

At a given temperature, the calculated rate constants for the four formulations tested exhibit a non-monotonic dependence of crosslinking reaction rates on composition. Below 97°C (the crossover temperature) $k$ decreases, depending on the formulation, as $1(0) > 7(67) > 3(33) > 9(100)$. This dependence may result, in part, from two competing effects: (1) a decrease in overall reaction rate with a decrease in the aromatic (higher $k$) epoxy and (2) an increase in reaction rate (as diffusion becomes important) with a decrease in formulation viscosity as aromatic content decreases. If the reaction rates are a non-monotonic function of composition, it is likely that network microstructure has a similar functional relationship with composition. Thus, a change in composition is not a simple increase or decrease in the weight per cent of a given pre-polymer, but a change in the three-dimensional network structure. If the aromatic component reacts sufficiently faster than the aliphatic epoxy, the aromatic epoxy novolac may be completely crosslinked before the aliphatic component has extensively reacted. In this case, the morphology would resemble that of an interpenetrating network (IPN)[10]. Thus, as we show below, the network structure (characterized by crosslink density) and the glass transition temperatures of these networks are non-linear functions of composition.

*Reaction mechanism.* As indicated above the reaction rates for the crosslinking reactions in epoxy formulations may be unambiguously obtained. However, the reaction mechanisms involved in the crosslinking of epoxides by various imidazole derivatives are, at present, only partially understood, and the final network structure depends on both rate and mechanism. Barton and Shepard[11] and Farkas and Ströhm[12] proposed that polymerization was initiated by reaction of the pyridine-type nitrogen (i.e. the unsubstituted nitrogen at the 3 position as shown in the structure of 1-(2-hydroxypropyl)-2-methylimidazole in *Figure 1*) with the epoxide group. Prior to polymerization a characteristic induction period was observed, with the induction time reflecting the rate of formation of a 1:1 imidazole/epoxy adduct. Further, it was argued that the imidazole is incorporated into the polymer in the subsequent polymerization. Recently, however, Ricciardi *et al.*[13] have established at least two pathways whereby, in principle, the original imidazole may be regenerated during the course of the reaction, such that imidazoles may function as true catalysts. Existing studies have yet to establish with certainty the extent to which regeneration occurs in the actual crosslinking of a multi-functional epoxy, particularly in the latter stages of polymerization. The rate of regeneration should also vary with the particular substituted imidazole derivative used as a catalyst, as well as its concentration. Although extractions on several cured compositions were performed using a variety of solvents such as tetrahydrofuran, acetone and water, no evidence of regenerated imidazole catalyst was detected. We shall adopt, therefore, the working hypothesis that 1-(2-hydroxypropyl)-2-methylimidazole is largely incorporated into the crosslinked polymer network, leaving open questions concerning the extent of its regeneration at various stages of cure.

If the imidazole curing agent used in this work is incorporated into the polymer, one possible pathway is via the 'Lewis Base' curing mechanism[14]. The primary crosslink points would then be ether linkages. In this case, the imidazole would be incorporated into the network at a carbon/nitrogen bond (at the 3 position) and it would function as a polar side chain. It is also possible, however, that after initial reaction of the imidazole and the epoxy to form an adduct, the hydroxypropyl group could form a network junction via an alkoxide intermediate. Detailed studies would be necessary to resolve these questions, and their resolution is beyond the scope of this work. In discussing the interpretation of the glassy state transitions ($\beta$-transitions) below, we will refer to motions involving the relaxation of the polar side chain hydroxypropylimidazole, assuming that the former of these two pathways for incorporation into the network is predominant.

*Variation of crosslink density with composition.* The parameter chosen to characterize the final network structure and relate it to macroscopic properties was crosslink density, which is, though indirectly, an experimentally accessible parameter. For the nine formulations, crosslink density decreased, generally, as the amount of aliphatic epoxy increased, with a maximum crosslink density for formulation 2(19) (*Figure 4*). Since it appears, overall, that the aliphatic epoxy reacts more slowly than the aromatic epoxy, it is reasonable that the extent of crosslinking (at a given temperature) decreases with the addition of aliphatic epoxy. It does not appear, however, that there is a direct correlation of reaction rate with degree of crosslinking. The maximum in crosslink density at formulation 2(19) may be accounted for by the decrease in viscosity with the addition of a small amount of aliphatic pre-polymer. At a given temperature, a lower viscosity would allow crosslinking of the aromatic epoxy to proceed further. At the same time, for such low levels of the aliphatic epoxy, its slower reaction rate would have a minimal effect on the overall conversion of the system.

### *Thermal transitions*

Both glass and $\beta$-transitions depend on molecular mobility, which, in turn, is a function of the chemical and/or physical nature of each molecule and its local environment. This is true whether the relaxational motions responsible for the transitions involve long or short chain segments, or side groups, and whether motion is cooperative or independent. In principle, then, the degree of crosslinking can affect $T_g$ and/or $T_\beta$ since the creation of network junctions, or tie points, can alter chain mobility. Also, the creation of these junctions usually forces the chains closer together, decreasing the volume available for the relaxational motion. For thermosets it has been shown[6,9,15–17] that the temperature, intensity and transition width of both the

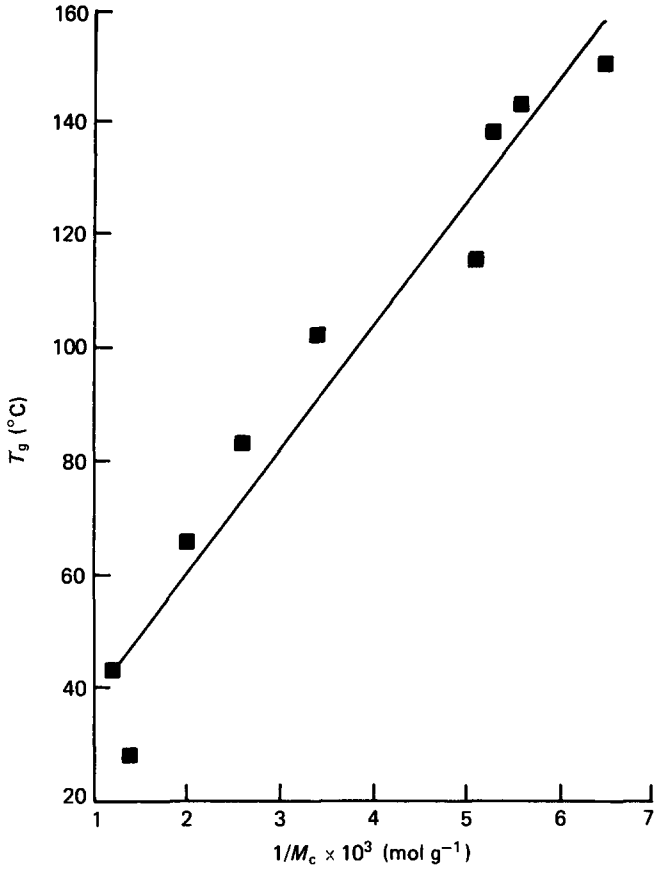


**Figure 9** Glass transition temperature vs. crosslink density

glass and $\beta$-transitions depend on crosslink density. In the current study, we have found a dependence of $T_g$ on the physical network structure, and of $T_\beta$ on chemistry.

*The glass transition.* Paralleling the decreases in $1/M_c$ discussed above, $T_g$ was found generally to decrease with increases in the aliphatic component (*Figure 5*). Also, *Figure 9* shows that for these materials, $T_g$ varies linearly with crosslink density, $1/M_c$. The slope of the line is $2.2 \times 10^4$. Neilsen[6] combined literature data to obtain the following empirical relation:

$$T_g = 3.9 \times 10^4/M_c + T_{g_o} \qquad (7)$$

where $T_{g_o}$ is the glass transition temperature of the uncrosslinked polymer*. The slopes obtained here and by Nielsen are of the same order of magnitude. With increasing crosslink density, molecular mobility decreases due to additional network tie points, and $T_g$ increases. This effect of crosslink density on $T_g$ is combined with, and is perhaps more important for networks of similar chemistry, than chemical effects.

*The $\beta$-transition. Figure 7* indicates that there is a systematic decrease in $T_\beta$ with increasing weight per cent of the aliphatic epoxy. At the same time, *Figure 4* shows that crosslink density is a non-monotonic function of the composition. Consequently, $T_\beta$ *versus* $1/M_c$ should be non-monotonic as well. This behaviour is evident in *Figure 10*, where $T_\beta$ is plotted against $1/M_c$ for 0.33, 3.0 and 30 Hz test frequencies. Thus, systematic changes in the chemical nature of the network, rather than physical changes (changes in $1/M_c$) *per se*, are responsible for changes in $T_\beta$.

It has been pointed out above that $E_{a,\beta}$ varies only slightly with composition, yet there is generally a 15°C to 20°C decrease in $T_\beta$ (for a given frequency) as the weight per cent of aliphatic epoxy increases. Since $E_{a,\beta}$ is roughly constant ($\pm 2.1$ kJ mol$^{-1}$), the molecular entity responsible for the transition is most likely the same, or very similar, for all the compositions. However, the molecular environment of the relaxing group varies with composition, and this gives rise to a variation in $T_\beta$ with composition. Specifically, the epoxy novolac network, with its aromatic rings, is relatively stiff compared to the network formed from aliphatic epoxy. This is evident in the stress/strain behaviour discussed below. There are numerous possibilities for rotation about carbon–carbon bonds for the aliphatic epoxy (see the structure in *Figure 1*). Networks formed from these two different pre-polymers exhibit considerable differences in response at a given temperature. Indeed, the large difference in $T_g$ (134°C for the aromatic vs. 28°C for the aliphatic epoxy) was already noted above. It may be expected, therefore, that the motion responsible for the $\beta$-transition would occur at lower temperatures, due to decreasing steric hindrance of the surrounding molecular environment, in those networks with higher amounts of the aliphatic component.

The role of network conformations in the $\beta$-relaxation can be further elucidated by calculating the entropy change, $\Delta S_\beta$, associated with the process. By comparing the simple Arrhenius relationship between frequency and activation energy with a corresponding relationship

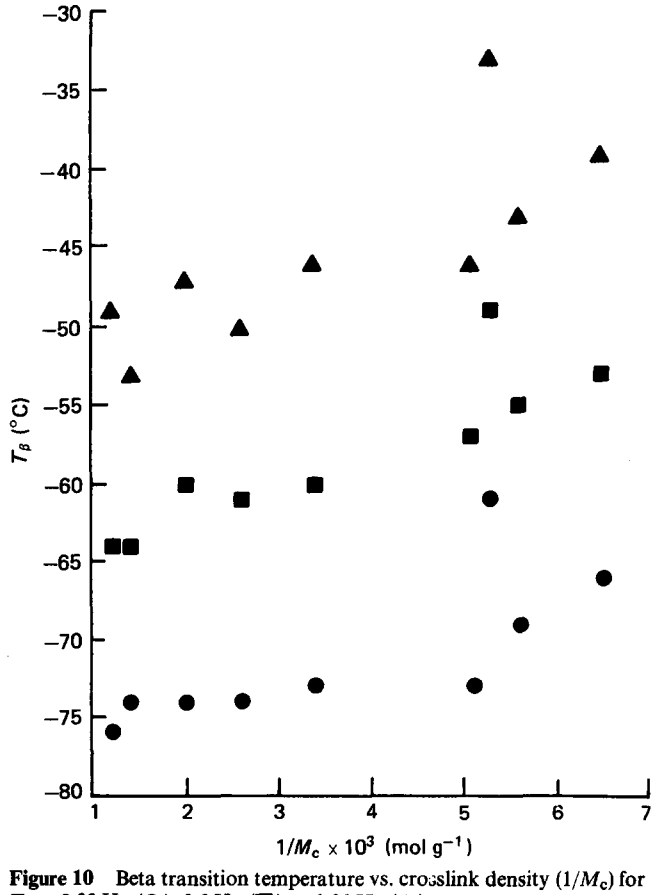


**Figure 10** Beta transition temperature vs. crosslink density ($1/M_c$) for $T_\beta$ at 0.33 Hz (●), 3.0 Hz (■) and 30 Hz (▲)

* For our systems, the intercept ($T_{g_o}$) was 14°C. However, this is a value for oligomeric pre-polymers, rather than uncrosslinked polymers, and cannot be compared with Neilsen's values of $T_{g_o}$.

derived from the theory of absolute reaction rates, Starkweather[18] has shown that at a frequency of 1 Hz,

$$E_{a,\beta} = RT_\beta[1 + \ln(kT_\beta/2\pi h)] + T_\beta \Delta S_\beta \quad (8)$$

Here, $T_\beta$ is the $\beta$-transition temperature at 1 Hz, $k$ is Boltzman's constant, $h$ is Planck's constant, and $R$ is the gas constant. A slight rearrangement of equation (8) gives

$$\Delta S_\beta = \frac{E_{a,\beta}}{T_\beta} - R[1 + \ln\{kT_\beta/2\pi h\}] \quad (9)$$

from which one may calculate activation entropies from measured activation energies (derived from Arrhenius plots) and transition temperatures. *Table 3* gives calculated values of $\Delta S_\beta$ as a function of composition.

It is clear, first of all, that $\Delta S_\beta > 0$ over the entire composition range. This means that the 'activated complex', i.e. the state through which the relaxing group plus surroundings must pass during the transition, is more disordered than the 'ground' state. This is the general case for viscoelastic relaxations, including the glass transition[18]. Secondly, as shown in *Figure 11*, $\Delta S_\beta$ decreases with increasing amounts of the aliphatic component. However, most of the decrease occurs in the 0 to 50% (formulations 1–5) composition range*.

Interestingly, the actual values for $E_{a,\beta}$, $\Delta S_\beta$ and $T_\beta$ fall within the range of values given by Starkweather[18] for the $\beta$-relaxation of polar groups in nylon-6 and poly(vinyl chloride). This is consistent with a mechanism involving the motion of a polar moiety in the cured network, although such a correspondence is not conclusive proof that motion of such a group is responsible for the transition. It was argued by Starkweather that non-zero activation entropies are indicative of cooperative motion, where the degree of cooperation increases with the magnitude of the entropy change. It would then follow from the variation of $\Delta S_\beta$ in *Figure 11*, that networks formed from the aromatic epoxy would require a greater degree of cooperative motion to accommodate the $\beta$-transition than the aliphatic networks. Thus, even though the actual energy required to carry out the $\beta$-transition is roughly equal for all of the networks, the degree to which the molecular environment must interact is greater for the aromatic than for the aliphatic systems.

In addition the magnitude of the $\beta$-transition, at a given frequency, was found to be independent of composition. This indicates that the number of relaxing groups is constant, even though the local molecular environment, as stated above, changes with composition. Since the amount of imidazole catalyst was approximately constant over the range of formulations and since the calculated entropies are consistent with the motion of a polar moiety, it is reasonable that the hydroxypropylimidazole catalyst, acting as a polar side chain, is the source of the $\beta$-relaxation.

*Macroscopic properties*

Crosslink density affects a range of network properties including moisture absorption[19,20], yield stress[21], tensile

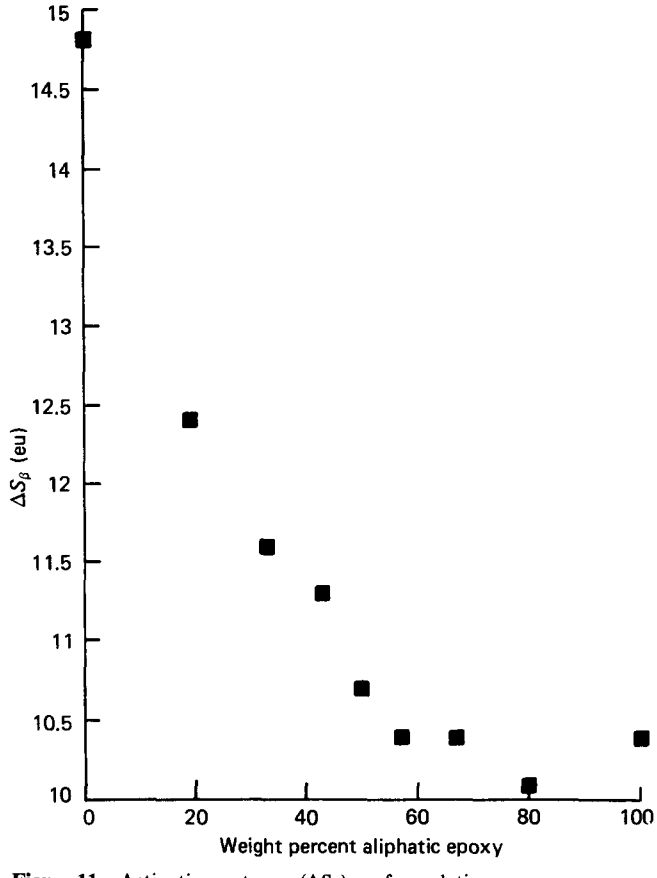


**Figure 11** Activation entropy ($\Delta S_\beta$) vs. formulation

modulus above $T_g$[6] (indeed, this dependence allowed us to calculate $1/M_c$), creep[6], density[19,20] and impact strength[22]. For the nine thermoset networks we have investigated the relationships between crosslink density and room temperature tensile modulus and break strength, room temperature toughness and yield, and impact behaviour.

*Room temperature modulus.* A plot of room temperature tensile modulus vs. crosslink density (*Figure 12*) shows that the modulus is roughly constant with the exception of formulation 9(100). This formulation has the second lowest crosslink density, $1/M_c = 1.4 \times 10^{-3}$ mol g$^{-1}$, but the minimum crosslink density is only slightly lower ($1.2 \times 10^{-3}$ mol g$^{-1}$). Considering that the glass transition actually occurs over a temperature range (up to $\pm 20$°C), and that formulation 9(100) has a $T_g$ only slightly above the measurement temperature (28°C), the material has probably become rubbery, accounting for the low modulus. On the other hand, formulation 8(80), which has the minimum crosslink density, has a $T_g$ about 20°C above the measurement temperature (44°C). Excluding formulation 9(100), then, it appears that the moduli of these networks are independent of crosslink density at room temperature (below $T_g$).

It has been reported previously[6] that the glassy state moduli of a series of chemically similar networks with different crosslink densities are independent of $1/M_c$. However, Chang *et al.* have found, for a series of networks formed from the diglycidyl ether of butanediol cured with 4,4′-diaminodiphenyl sulphone, that the tensile modulus increased with crosslink density[9]. They attributed the modulus increase to an increase in room temperature

* The values for $\Delta S_\beta$ shown in *Figure 11* were calculated from equation (9) using the mean activation energy 65.1 kJ mol$^{-1}$. Corresponding calculations using the individual values of $E_{a,\beta}$ in *Table 3* show the same trend, but with considerable scatter for compositions in the 50 to 100% range (formulations 5–9).

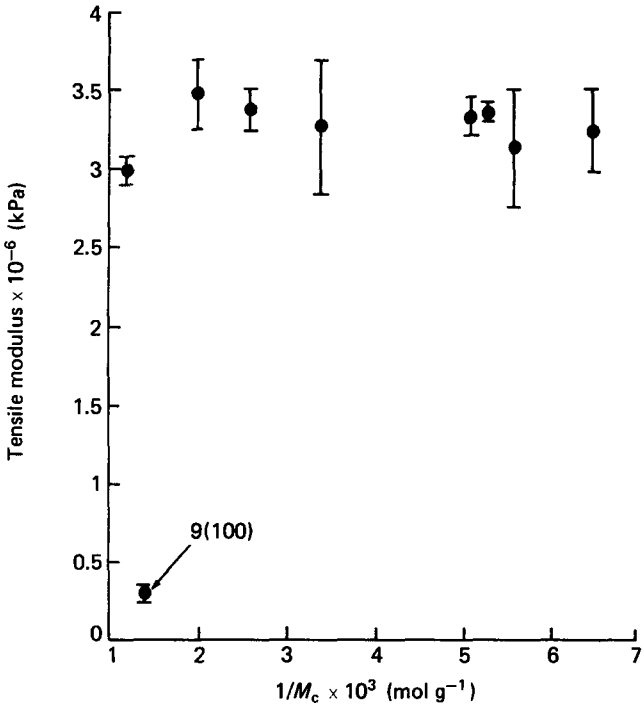


**Figure 12** Tensile modulus vs. crosslink density ($1/M_c$)

bulk density, that is, a more tightly packed network is obtained with increasing $1/M_c$. For our systems the room temperature bulk densities, with the exception of formulation 9(100), were constant. Thus, our results, if room temperature tensile moduli are a function of bulk density, are in accord with Chang's[9] results since both tensile moduli and bulk density are constant. For this epoxy novolac system, the bulk density, or packing, is apparently not greatly affected by crosslink density. Gupta *et al.* have recently stated[20] that intermolecular packing is the key factor determining room temperature tensile modulus, a low-strain property.

*Tensile strength.* Tensile strength, as opposed to tensile modulus, is a high-strain property, and consequently should vary with crosslink density (*Figure 13*). As $1/M_c$ increases from formulation 9(100), break strength increases until formulation 5(50). As crosslink density continues to increase with formulations 4(43)–1(0), break strength drops off slowly. As the material changes from a lightly crosslinked, rubbery material to a more densely crosslinked, rigid material, mechanical integrity and the ability to sustain load increase. However, at very high crosslink densities, other factors come into play. Tensile strength is a flaw sensitive property[20]. Flaws may be extrinsic, such as air voids, or intrinsic to the network itself. In formulations with greater amounts of the aromatic epoxy, initial viscosity is high and probably increases rapidly with the crosslinking reaction. As viscosity increases, and the reactive species become less mobile, they cannot diffuse evenly throughout the reaction mixture. Thus, where there are high concentrations of reactive groups, it is possible that regions of high crosslink density occur. On the other hand, where there are few reactive species, regions of low crosslink density may occur. The growing network can thereby become heterogeneous, creating a distribution of $1/M_c$ and, therefore, $M_c$. An increasing number of internal, or structural, flaws (regions of low crosslink density) would then result in a decrease in tensile strength. A high level of flaws in the test samples would also account for the scatter in the tensile data for formulations containing high levels of aromatic epoxy.

*Toughness.* Room temperature toughness (obtained from tensile load vs. elongation curves), another high-strain property, also changes with crosslink density, exhibiting a maximum at $1/M_c = 2.6 \times 10^{-3}$ mol $g^{-1}$ (formulation 6(57)). This is shown in *Figure 14*. The highly crosslinked, predominantly aromatic formulations 1(0)–4(43) exhibit low toughnesses, as do the lightly crosslinked, predominantly aliphatic formulations 7(67)–9(100). It is the formulations with intermediate levels of

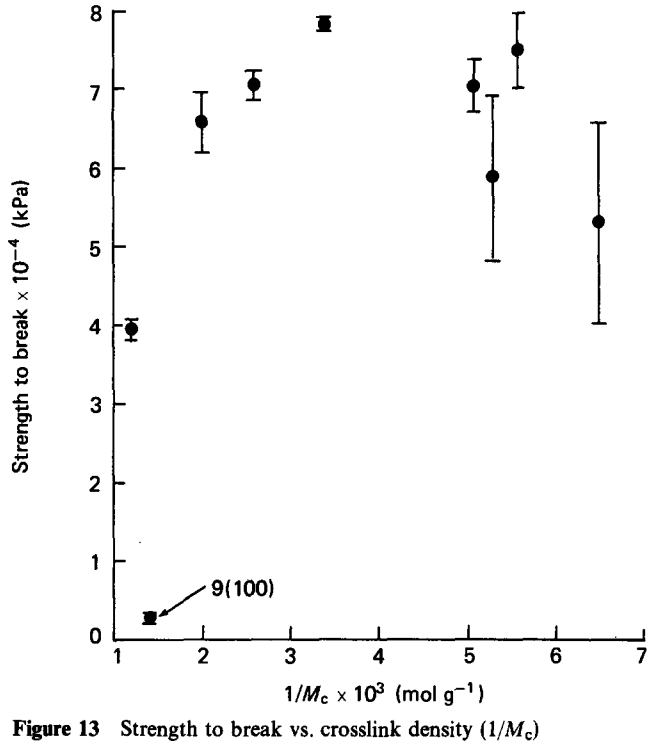


**Figure 13** Strength to break vs. crosslink density ($1/M_c$)

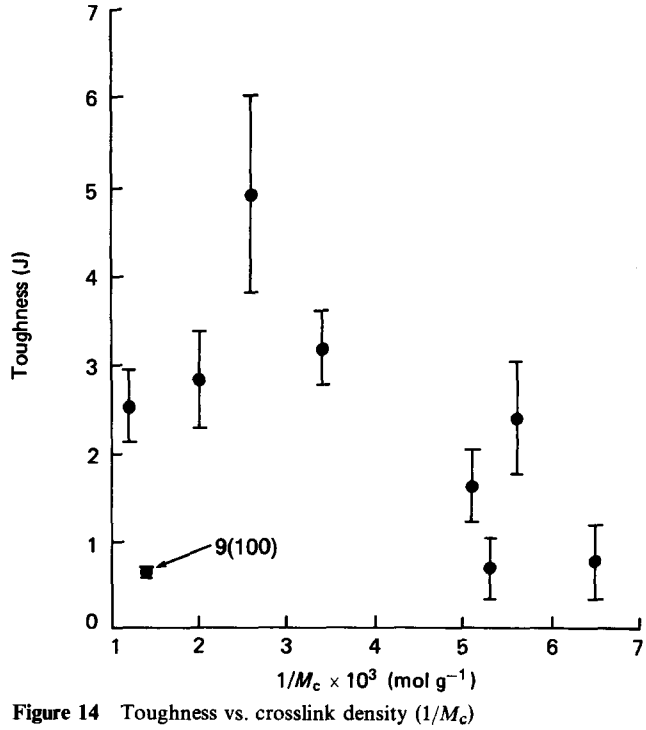


**Figure 14** Toughness vs. crosslink density ($1/M_c$)

crosslinking and equal, or almost equal, amounts of the two epoxy components, e.g. 6(57), which have the maximum toughness. Toughness appears to require a combination of the properties characteristic of each of the high and low crosslink density formulations: high modulus and yielding (plastic deformation), respectively. While all formulations, except 9(100), have comparable moduli, (3.0–3.5 kPa), the highly crosslinked materials fail in a brittle manner, whereas the lightly crosslinked materials yield prior to break. The yield points for formulations 6(67)–8(80) are given in *Table 5*. Although formulation 9(100) did not exhibit a load drop with increasing elongation, the load vs. elongation curve was highly non-linear. *Figure 15*, which shows traces of load vs. elongation for formulations 1(0), 6(57) and 9(100), illustrates that the combination of high modulus with extensive yield produces high toughness, i.e. the greatest area under the curve. The formulation 9(100) sample did eventually break (out of range of this Figure). Brittle failure in formulations 1(0)–4(43) results from network flaws, the stiffness of the aromatic molecules, and the high level of crosslinking which prevents inter- and intramolecular mobility. Plastic yielding can occur in the less crosslinked materials since a greater degree of segmental mobility is allowed.

The toughness of a material depends on the ability of that material to absorb, or dissipate, energy (impact, or other). This requires chain mobility, as noted above. The energy absorbing mechanism in the glassy state which has been associated with impact and toughness behaviour is the $\beta$-transition[22,23]. Specifically, if the $\beta$-transition occurs at the temperature and frequency of impact, the impact energy can be absorbed. An alternative interpretation says that, for static conditions, better impact properties are obtained with lower values of $T_\beta$. As the relaxation is traversed from below, volume becomes available for chain motion. At temperatures above $T_\beta$ (but

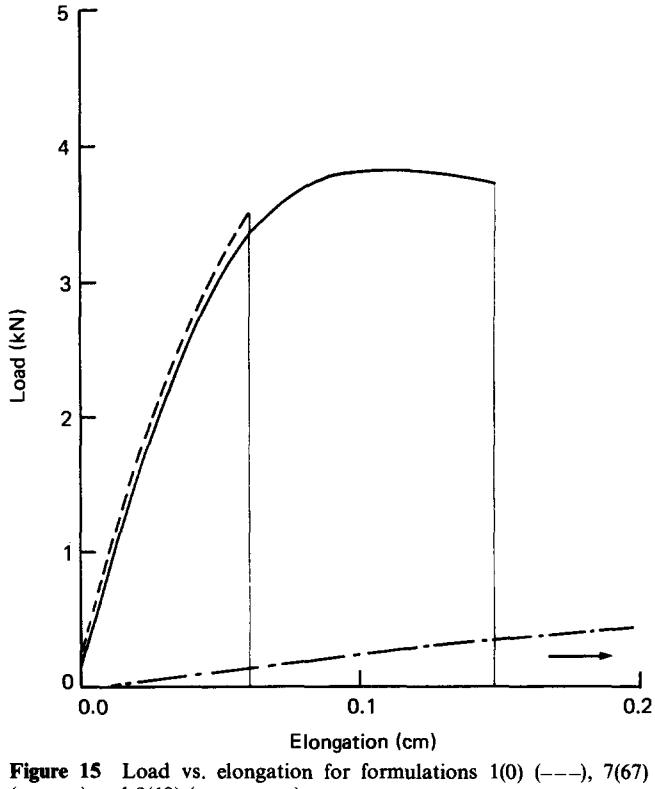


**Figure 15** Load vs. elongation for formulations 1(0) (– – –), 7(67) (———) and 9(10) (— — — —)

**Table 6** Room temperature $\beta$-transition frequency

| Formulation | $T$ (K) | $\log f_{\beta,RT}/f_{\beta,T}$[a] | $\log f_{\beta,RT}$ | $f_{\beta,RT}$ (Hz × $10^4$) |
|---|---|---|---|---|
| 1(0) | 233 | 3.330 | 4.330 | 2.138 |
| 2(19) | 227 | 3.602 | 4.602 | 3.999 |
| 3(33) | 224 | 3.775 | 4.775 | 5.957 |
| 4(43) | 221 | 3.865 | 4.865 | 7.328 |
| 5(50) | 219 | 4.027 | 5.027 | 10.64 |
| 6(57) | 218 | 4.335 | 5.335 | 21.63 |
| 7(67) | 217 | 4.272 | 5.272 | 18.71 |
| 8(80) | 217 | 4.016 | 5.016 | 10.38 |
| 9(100) | 217 | 4.357 | 5.357 | 22.75 |

[a] $f_{\beta,T} = 10$ Hz; $T_{RT} = 298$ K

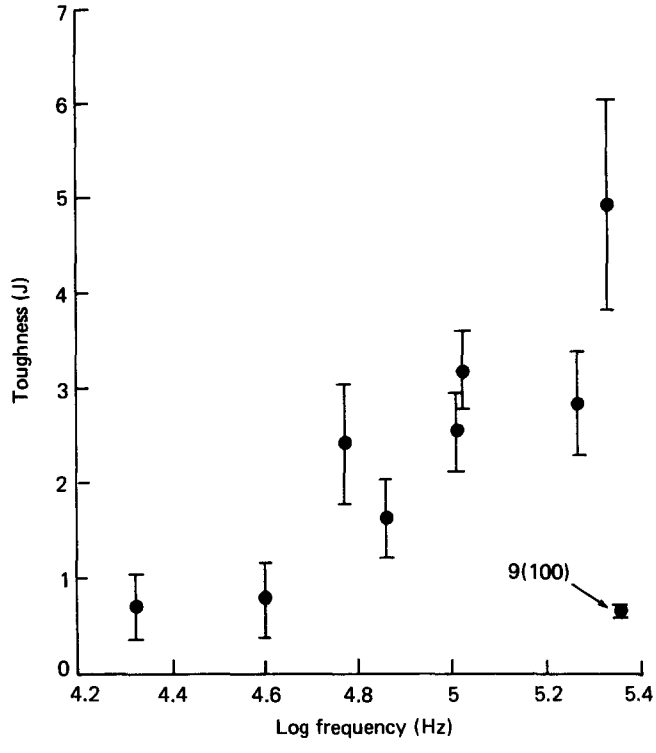


**Figure 16** Toughness vs. room temperature frequency of the beta transition

below $T_g$) energy can be absorbed to a greater extent than below $T_\beta$.

A relationship between the room temperature frequency of the $\beta$-transition, $f_{\beta,RT}$, and toughness, where toughness increases with increasing $f_{\beta,RT}$, has been described by Boyer[24]. The room temperature frequency of the $\beta$-transition can be calculated from:

$$\log(f_{\beta,T}/f_{\beta,RT}) = (E_{a,\beta}/2.3R)\left(\frac{1}{T} - \frac{1}{T_{RT}}\right) \qquad (10)$$

where $E_{a,\beta}$ is the activation energy of the $\beta$-relaxation, $f_{\beta,T}$ is the frequency of the transition at some temperature $T$, $R$ is the gas constant, and $T_{RT}$ is 298 K. From the temperatures and frequencies of the $\beta$-transition listed in *Table 5*, and the activation energies listed in *Table 3**, $f_{\beta,RT}$ was calculated for each formulation (*Table 6*).

Toughness vs. log $f_{\beta,RT}$ is plotted in *Figure 16*. With the exception of formulation 9(100), a general trend of increasing toughness with increasing log $f_{\beta,RT}$ was observed. Boyer[24] has suggested that this relationship

* The values of $f_{\beta,RT}$ were calculated from equation (10) using each $E_{a,\beta}$. Corresponding calculations using the mean $E_{a,\beta}$ (61.5 kJ mol$^{-1}$) show the same trend, but with greater scatter.

should hold only if the $\beta$-transition arises from the main chain motion, the implication being that more volume is required for, and therefore available after, main chain relaxations. Additionally, main chain relaxations would have a higher activation energy and be able to absorb more energy. Despite this, the relationship between toughness and $\beta$-relaxation appears to hold here, even though we have attributed the relaxation to motion of a hydroxypropylimidazole side chain. However, according to our earlier discussion of the entropy change involved in the $\beta$-relaxation, a high degree of interaction with the main network chains is required for the $\beta$-relaxation to occur.

## CONCLUDING REMARKS

Although the kinetics and mechanism of the complicated crosslinking reactions are not completely understood, we have been able to obtain structural information for a series of thermoset networks based on aromatic/aliphatic epoxy mixtures. Crosslink density and $T_g$ decreased as the amount of aliphatic epoxy increased. $T_g$ exhibited a linear dependence on crosslink density. However, the $\beta$-relaxation depended on chemical composition rather than crosslink density, and $T_\beta$ decreased with increasing amounts of the aliphatic epoxy. The $\beta$-transition, for all formulations, was attributed to the relaxation of a polar moiety. Composition, crosslink density, bulk density, and $T_\beta$ also play a role in determining, for example, moisture uptake and diffusion through glassy networks. In turn, use temperature is affected since increasing moisture content will increasingly plasticize the network and decrease $T_g$ as well as the modulus.

We have also related mechanical behaviour to structural properties for these materials. While the sub-$T_g$ modulus was independent of crosslink density, but was found to depend on bulk density, tensile strength and toughness were functions of crosslink density. Tensile toughness also exhibited a correlation with the $\beta$-relaxation. The dependence of impact toughness in the $\beta$-relaxation was described as well.

## ACKNOWLEDGEMENTS

The authors would like to thank William R. Lee for performing the d.s.c. and DMA measurements. We are grateful to Drs T. S. Ellis, Z. G. Gardlund and H. G. Kia for helpful discussions, to R. P. Schuler for the high temperature equilibrium moduli measurements, and to Mark A. Myers for n.m.r. measurements.

## REFERENCES

1 Kissinger, H. E. *Anal. Chem.* 1957, **29**, 1702
2 Rogers, R. N. and Smith, L. C. *Anal. Chem.* 1967, **39**, 1024
3 Lemay, J. D., Swetlin, B. J. and Kelley, F. N. in 'Characterization of Highly Crosslinked Polymers', (Eds. S. S. Labana and R. A. Dickie), American Chemical Society, Washington, D.C., 1984
4 Aklonis, J. J., Macknight, W. J. and Shen, M., 'Introduction to Polymer Viscoelasticity', Wiley–Interscience, New York, 1972, Ch. 6
5 Treloar, L. R. G., 'The Physics of Rubber Elasticity', Clarendon Press, Oxford, 1958
6 Nielsen, L. E. *J. Macromol. Sci.–Revs. Macromol. Chem.* 1969, **C3(1)**, 69
7 Takahama, T. T. and Geil, P. H. *J. Polym. Sci., Polym. Lett. Edn.* 1982, **20**, 453
8 Read, B. E. *Polymer* 1981, **22**, 1580
9 Chang, T. D., Carr, S. H. and Brittain, J. O. *Polym. Eng. Sci.* 1982, **22**(18), 1205
10 Frisch, H. L. *Br. Polym. J.* 1985, **17**(2), 149
11 Barton, J. M. and Shepherd, P. M. *Makromol. Chem.* 1975, **176**, 919
12 Farkas, A. and Ströhm, P. F. *J. Appl. Polym. Sci.* 1968, **12**, 159
13 Ricciardi, F., Romanchick, W. A. and Joullie, M. M. *J. Polym. Sci., Polym. Chem. Edn.* 1983, **21**, 1475
14 Lee, H. and Neville, K., 'Handbook of Epoxy Resins', McGraw–Hill Co., New York, 1967, pp. 4–5
15 Banks, L. and Ellis, B. *Polymer* 1982, **23**, 1466
16 Meares, P., 'Polymers: Structure and Bulk Properties', VanNostrand Co., Ltd., New York, 1965, p. 265
17 Ward, I. M., 'Mechanical Properties of Solid Polymers', Wiley–Interscience, New York, 1971, pp. 171–172
18 Starkweather, H. W. *Macromolecules* 1981, **14**, 1277
19 Diamont, Y., Marom, G. and Broutman, L. J. *J. Appl. Polym. Sci.* 1981, **26**, 3015
20 Gupta, V. B., Drzal, L. T., Lee, C. Y.-C. and Rich, M. J. *Polym. Eng. Sci.* 1985, **25**(13), 812
21 Morgan, R. J., Kong, F.-M. and Walkup, C. M. *Polymer* 1984, **25**, 375
22 Timm, D. C., Ayorinde, A. J. and Foral, R. F. *Br. Polym. J.* 1985, **17**(2), 227
23 Sacher, E. *J. Appl. Polym. Sci.* 1975, **19**, 1421
24 Boyer, R. F. *Polymer* 1976, **17**, 996